Available online at www.sciencedirect.com
ScienceDirect
Journal of Membrane Science 285 (2006) 166–172
journal of MEMBRANE SCIENCE
www.elsevier.com/locate/memsci

Gas permeation properties of poly(lactic acid) revisited

Lihong Bao [a], John R. Dorgan [b,*], Dan Knauss [c], Sukendu Hait [c], Nelson S. Oliveira [d], Isabel M. Maruccho [d]

[a] *Chembrane Research and Engineering Inc., Newark, NJ 07103, USA*
[b] *Chemical Engineering Department, Colorado School of Mines, Golden, CO 80401, USA*
[c] *Chemistry Department, Colorado School of Mines, Golden, CO 80401, USA*
[d] *CICECO, Department de Quimica, Universidade de Aveiro, 3810-193 Aveiro, Portugal*

Received 10 April 2006; received in revised form 21 August 2006; accepted 22 August 2006
Available online 26 August 2006

Abstract

Pure gas permeation through solution-cast amorphous poly(lactic acid) (PLA) films is investigated using the time-lag method. New data on permeability, diffusivity and solubility for N_2, O_2 and CO_2 are reported. At 30 °C, N_2 permeability, diffusivity and solubility in PLA (98.7% *L*, 1.3% *D*) are 0.05 Barrer, 2.4×10^{-8} cm^2/s, and 2.2×10^{-4} cm^3 (STP)/cm^3 (polymer) cmHg. The measured activation energy of N_2 permeation is 34.6 kJ/mol. For O_2, the corresponding values are 0.26 Barrer, 5.7×10^{-8} cm^2/s, 4.9×10^{-4} cm^3 (STP)/cm^3 (polymer) cmHg and 24.0 kJ/mol. The values for CO_2 are 1.10 Barrer, 4.4×10^{-9} cm^2/s, 0.025 cm^3 (STP)/cm^3 (polymer) cmHg and 18.0 kJ/mol. These new measurements of the gas permeation properties of poly(lactic acid) (PLA) show considerable disagreement with previously reported results [H.J. Lehermeier, J.R. Dorgan, J.D. Way, Gas permeation properties of poly(lactic acid), J. Membr. Sci. 190 (2001) 243–251] obtained using a continuous flow apparatus. The effect of PLA optical compositions on permeation is also investigated and found to be consistent with the earlier report; the *L*/*D* ratio has no effect on the permeation properties provided the material is quenched into an amorphous state. The ability to generate diffusivity and solubility data along with the greater sensitivity of pressure measurement over gas composition argues in favor of the use of the time-lag apparatus for pure gas permeability measurements and suggests that the revised PLA permeation values reported here should be adopted.

Keywords: Poly(lactic acid); Gas Permeation; Time-lag; Solubility; Diffusivity; Activation energy

1. Introduction

Poly(lactic acid) (PLA) has received increased attention in the last decade due to its natural biodegradability and availability from renewable resources[1,2]. PLA can replace hydrocarbon-based polymers such as polystyrene in certain packaging applications and can also be used as a textile material. Full-scale commercial production of PLA is now a reality; the cost of production has been reduced significantly and PLA is being used in diverse applications such as fibers, films, and packaging [3,4]. Therefore, there is a continuing need for a clear understanding of the gas permeation properties of PLA.

PLA is reportedly a relatively poor barrier to water vapor and CO_2. The water–vapor transmission rate of PLA is significantly higher than for PET, PP or PVC [5]. Recently, Auras et al. [6] investigated barrier properties of two biaxially oriented PLA films (NatureWorks LLC PLA 4030-D and PLA 4040-D). The stereochemical content of PLA 4030-D is 98%-*L* for PLA4040-D, it is 94% *L*. CO_2 permeability in PLA 4030-D at 25 °C is reported as 1.9 Barrers and activation energy of permeation is 15.65 kJ/mol; in PLA 4040-D, the values are 1.4 Barrers and 19.44 kJ/mol. O_2 permeability in PLA 4030-D at 25 °C is reported as 0.11 Barrers and permeation activation energy is 41.43 kJ/mol; in PLA 4040-D, the values are 0.13 Barrers and 28.43 kJ/mol. NatueWorks LLC, a PLA manufacturer, reports barrier properties of its biaxially oriented films as follows: the permeability of O_2 is 550 cm^3 mil/m^2 day atm (∼0.21 Barrers), the CO_2 permeability is 3000 cm^3 mil/m^2 day atm (∼1.2 Barrers) [7].

In a previous work, the permeation of nitrogen, oxygen, carbon dioxide and methane in very thin (5 μm) amorphous films of various grades of PLA (*L*:*D* ratios from 95:5 to 98:2) cast

* Corresponding author. Tel.: +1 303 273 3539; fax: +1 303 3730.
E-mail address: jdorgan@mines.edu (J.R. Dorgan).

0376-7388/$ – see front matter © 2006 Elsevier B.V. All rights reserved.
doi:10.1016/j.memsci.2006.08.021

Table 1
Polylactide properties

Sample no.	L (%)	D (%)	M_n (g/mol)	M_w (g/mol)	T_g (°C)
270-60-3	98.7	1.3	[a]	1.90E+5	59
SH-PLA-19	80	20	9.25E+4	1.42E+5	54
SH-PLA-43	50	50	8.40E+4	1.72E+5	52

[a] Not available.

from solution was examined using a flow through geometry and gas chromatography detection [8]. N_2 permeability in PLA was reported as 1.3 Barrers at 30 °C, and the N_2 permeation activation energy is 11.2 kJ/mol. For O_2 the corresponding values are 3.3 Barrers and 11.1 kJ/mol, and the reported values for CO_2 permeation are 10.2 Barrers and 6.1 kJ/mol. It was also shown that changes in polymer chain branching and L:D ratios have no effect on the permeation properties of small gases. However, compared to the more recent studies cited in the last paragraph, these permeabilities are about an order of magnitude higher. Also no diffusivity or solubility data for gases in PLA have ever been reported. Thus, there exists a need to carefully examine the existing data, present new independent measurements, and come to consensus values for the permeation properties of PLA. In addition, diffusivity or solubility data are desirable. Finally, the L:D ratios of the PLA samples reported on to date were limited to a very small range. This paper thus revisits permeation properties of PLA in order to: (1) rectify the discrepancy in permeability data; (2) find diffusivity and solubility data for gases in PLA; (3) investigate the effects of L:D ratios on the permeation over a wider range.

2. Experimental

2.1. Materials

PLA used in the experiments were obtained from two sources. Table 1 gives the manufacturers, L:D content, molecular weight, and glass transition temperatures (T_g). The SH-PLAs were synthesized using stannous octanoate-catalyzed ring-opening polymerizations. L-Lactide and D-lactide (Purac Biochem, Holland) were crystallized from toluene. Tin-2-ethylhexanoate (Aldrich Chemical Co., USA) was distilled under vacuum before use. Benzyl alcohol (Aldrich Chemical Co., USA) was dried with CaO and distilled under reduced pressure. All polymerizations were performed using the following procedure, with different ratios of L- to D-lactide and amounts of benzyl alcohol.

Lactide (50 g, 0.347 mol) and $Sn(Oct)_2$ (5.63 mg, 0.138 mmol) were added to a 50 mL round-bottom flask, dried under vacuum for 4 h, sealed under a rubber septum, and then purged with argon for 20 min. Benzyl alcohol (required amount) was added using a syringe. The polymerization reaction was performed by heating the vessel at 130 °C for 12 h under argon atmosphere, with magnetic stirring. The resulting polymer was dissolved in dichloromethane, precipitated with a 10-fold excess of hexane, and dried under reduced pressure (1 Torr) for 48 h.

Reagent grade methylene chloride that was 99.6% pure was obtained from Aldrich and used as received for the solvent for membrane casting.

High purity gases were used to ensure accuracy of the data. N_2 was 99.999% pure; CO_2 was 99.99% pure; and O_2 was 99.993% pure. All gases were obtained from General Air.

2.2. Methods

PLA films were cast from a 10 wt.% solution in methylene chloride using a Gardner casting blade onto a glass plate. Solvent was slowly evaporated for several hours from the film, sometimes with the aide of a cover. Films were subsequently floated off the glass plate onto a water surface, recovered, and dried overnight in a vacuum oven at room temperature.

Various methods for measuring permeability of polymer films have been described in the literature. The time-lag method [9], which allows measurement of permeability, diffusivity and solubility data simultaneously, is used and described as following.

An apparatus for the measurement of the pure gas permeation properties in polymeric membranes was built in the lab. The apparatus set-up is best described by categorizing it into two subsystems. One is the gas-control subsystem, including feed gas supply, gas regulatory system (valves), membrane holder, temperature control (oven), constant volume cylinder and vacuum pump. The other is data acquisition and control subsystem, including all the sensors (temperature and pressure), data acquisition card, valve-control relays, and the Labview program. Fig. 1 shows the diagram of the gas-control subsystem.

The film is degassed under vacuum for between 12 and 16 h. Penetrant gas is then introduced on the upstream side at constant pressure (p_f). Depending on the rate of permeation of a given sample variable downstream volumes may be affixed. Under these conditions, the amount of permeant per unit area that has permeated through the membrane, Q_t, is given by

$$\frac{Q_t}{Lc_f} = \frac{Dt}{L^2} - \frac{1}{6} - \frac{1}{\pi^2}\sum_{n=1}^{\infty}\frac{(-1)^n}{n^2}\exp\left[-\frac{Dn^2\pi^2 t}{L^2}\right] \quad (1)$$

where L is the membrane thickness, c_f the upstream concentration, D the diffusivity, and t is the time. Assuming equilibrium at the upstream interface and that the gas concentration is low enough that Henry's law is valid, gives

$$c_f = Sp_f \quad (2)$$

where S is the Henry's law coefficient or solubility. Using the ideal gas law:

$$p_p V_p = (Q_t A)RT \quad (3)$$

where p_p and V_p refer to the downstream pressure and volume, respectively, and A is the area of the membrane. Accordingly, Q_t is obtained from measurement of p_p as a function of time. The existence of highly sensitive pressure transducers that provide excellent response gives this technique considerable advantage.

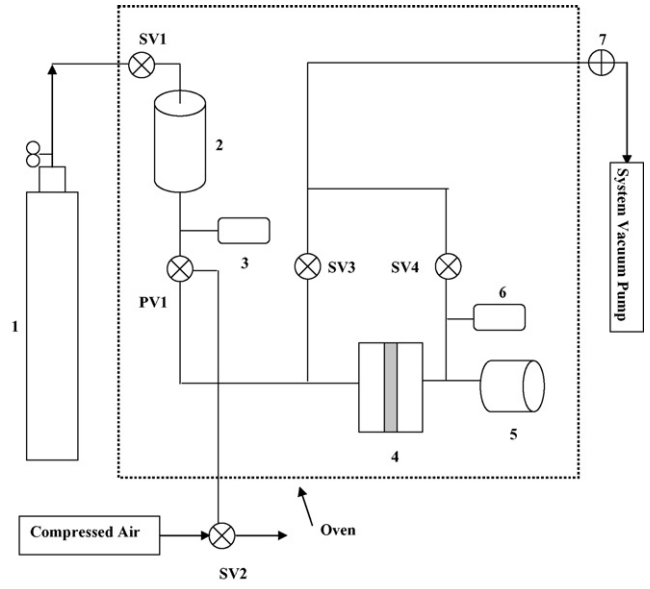

Note: 1 --- Gas Cylinder
2 --- Feed Gas Volume Cylinder
3 --- Feed-side Pressure Transducer
4 --- Membrane Holder
5 --- Permeate-Gas Volume Cylinder
6 --- Permeate-side Pressure Transducer
7 --- 3-way Manual Valve
SV1-4 --- Solenoid Valves
PV1--- Pneumatic Valve

Fig. 1. Diagram of the time-lag apparatus.

At longer times, Eq. (1) can be written as

$$\frac{LQ_t}{p_f} = DS\left(t - \frac{L^2}{6D}\right) = P\left(t - \frac{L^2}{6D}\right) \quad (4)$$

where P is the permeability, defined as the product of diffusivity and solubility. When LQ_t/p_f is plotted against time t based on Eq. (4), the asymptote of the resulting curve makes an intercept of $L^2/6D$ on the t axis and has a slope of P. This intercept on the t-axis is the time lag, θ. Knowing D and slope, P, allows calculation of solubility, $S = P/D$.

The error associated with the measurement comes from various sources, such as the accuracy of pressure transducer and temperature sensor, leaking, membrane thickness, etc. An estimation of the experimental error can easily be done through uncertainty principle. The relative error of permeability was found to be less than 5% for higher permeability measurement, about 7% for permeability close to lower limit. The relative error of diffusivity, dependent on membrane uniformity and time lag, was in the range of 4–12%. As a result, the relative error of solubility would be in the range of 6–14%.

3. Results and discussion

3.1. LDPE permeation

As a means of verification of the time-lag apparatus, N_2 permeation in blown LDPE films provided by Dow chemical was measured. The membrane thickness is 210 μm. Data are shown in Fig. 2. The measured N_2 permeability and diffusivity at 25 °C are 0.90 Barrer and 3.6×10^{-7} cm^2/s. The permeation activation energy is 49.6 kJ/mol. The corresponding literature values are 0.97 Barrer, 3.2×10^{-7} cm^2/s and 49.4 kJ/mol, respectively [10]. These measured values are in very good agreement with established literature values.

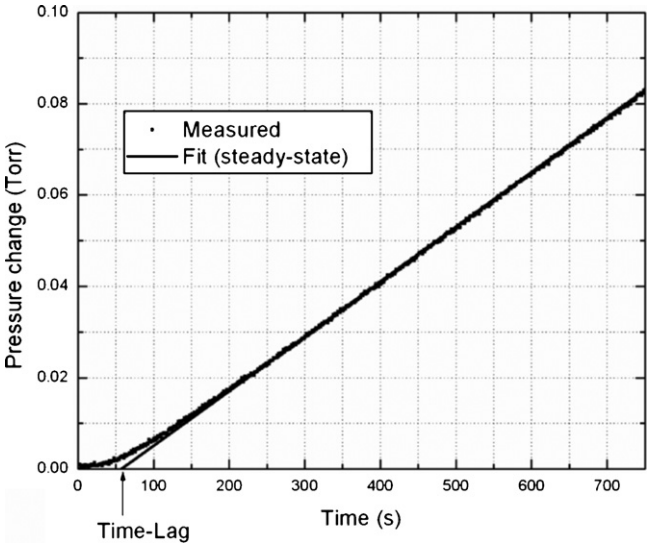

Fig. 2. Typical time lag for N_2 permeation in LDPE. The measurement was conducted as a verification of the apparatus.

3.2. PLA film annealing

It is well known that gas permeation and sorption properties of glassy and amorphous polymers are particularly sensitive to the film preparation protocol and physical aging [11]. PLA has a relatively low glass transition temperature near 55 °C (see Table 1) and is known to undergo significant physical aging at room temperature. When films physically age, the permeability decreases. This is generally associated with increasing densification and decreasing free volume. Verification of reproducibility during preliminary stages of this work demonstrated that PLA permeability decreases gradually with time reflecting physical aging. Accordingly, a procedure was developed to investigate the aging effects on the permeation. The PLA film was prepared as described in Section 2.2 and then permeation measurements were carried out as temperature was increased from room temperature to about 45 °C. The PLA film was then annealed at a temperature 5 °C below its glass transition temperature for 12 h. After annealing, permeation measurements are taken in a temperature cycle from higher (~45 °C) to lower (ambient) and back to the higher temperature. Fig. 3 shows the measured CO_2 permeability in PLA film (L:D = 98.3:1.7) during this procedure. It can be easily seen that annealing gives a decrease in permeability of around 20%. Optical microscopy showed no evidence of increased crystallinity as a result of this sub-T_g annealing process. Annealing leads to path independent and reproducible results. Therefore, all the results reported in the paper are from films annealed according to this procedure.

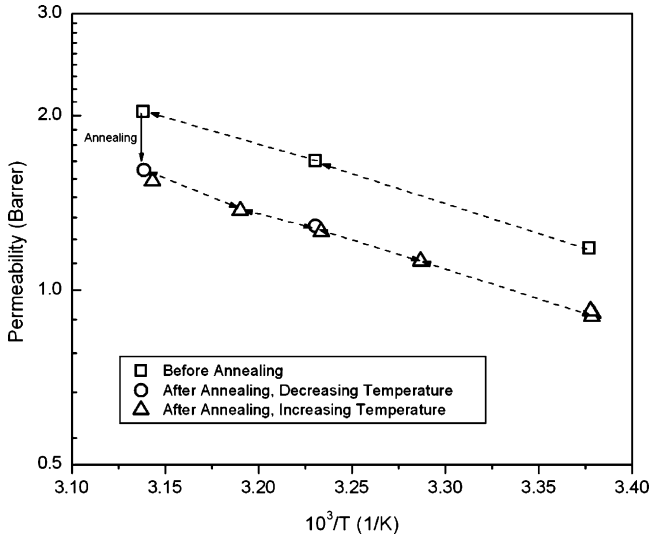

Fig. 3. The measured CO_2 permeability in PLA film (L:D = 98.3:1.7) during annealing procedure.

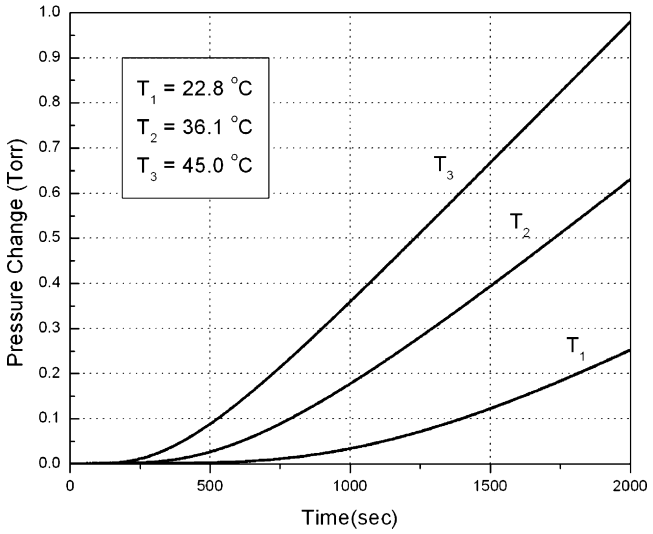

Fig. 4. Typical time lags for CO_2 permeation in PLA (L:D = 98.7:1.3) under different temperatures.

3.3. Film crystallinity

Besides physical aging and polymer thermal history, the diffusion and sorption of gases in semi-crystalline polymers depends on many other factors, such as polymer-gas molecule chemistry, free volume in the amorphous phase and crystallinity. All films used in this work were checked for evidence of crystallinity by optical microscopy and differential scanning calorimetry (DSC). For L:D = 98.7:1.3, films showed evidence of a small degree of crystallinity under cross-polarized light both before and after annealing. DSC confirmed that less than 4% crystallinity exists in these films. A high crystallinity PLA (L:D = 98.7:1.3) film was made by annealing under vacuum at 110 °C for 24 h and used for comparison, crystallinity was very apparent the microscope and DSC showed 40+% crystallinity. It can be concluded that films before and after the permeation tests have a very small crystallinity; this finding is consistent with the previous measurements [8]. For PLA films (L:D = 80:20 and 50:50), no crystallites were found, consistent with a totally amorphous material.

3.4. CO_2 permeation

A typical time-lag data for carbon dioxide (CO_2) permeation in PLA (L:D = 98.7:1.3) with thickness of 50.5 μm under different temperatures are shown in Fig. 4. Three measurements are conducted, and the standard deviation is 0.08. Films with different L:D ratio and thickness are used, and the time lags are in the range of 450–1300 s allowing CO_2 diffusivity to be easily measured with good accuracy. As the temperature increases, the lag time becomes shorter, which means the diffusivity increases with temperature. According to Eq. (1), steady-state conditions are reached after a period amounting to two to three multiples of the time lag. All the experiments leading to the results reported here were carried out for at least five or six multiples of the time lag.

Figs. 5–7 detail the temperature dependence of CO_2 permeation in PLA having an L:D ratio of 98.7:1.3. Fig. 5 shows the temperature dependence of CO_2 permeability. At 30 °C, the permeability is 1.1 Barrers; permeability increases with temperature. A very good linear relationship between ln P and 1/T is obtained. Error analysis based on the uncertainties in the measured variable provides the error bars shown in the plot. The activation energy for CO_2 permeation is 18.5 kJ/mol, which is three times larger than previous value, but close to Auras's value. Fig. 6 shows the temperature dependence of CO_2 diffusivity. At 30 °C, CO_2 diffusivity is 4.4×10^{-9} cm^2/s. Diffusivity also increases with temperature and a good linear relationship exists between ln D and 1/T. The corresponding activation energy of diffusion is 36.7 kJ/mol. Temperature dependence of CO_2 solubility, determined from the time-lag experiment, is shown in Fig. 7. Solubility decreases with temperature as expected. At

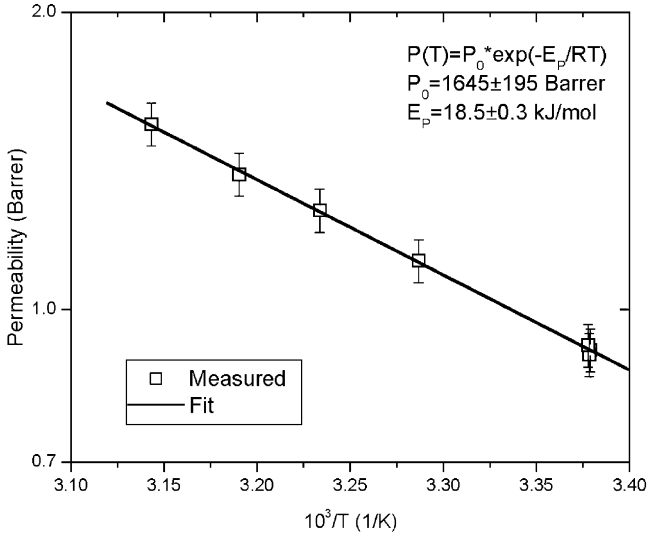

Fig. 5. Temperature dependence of CO_2 permeability in PLA (L:D = 98.7:1.3).

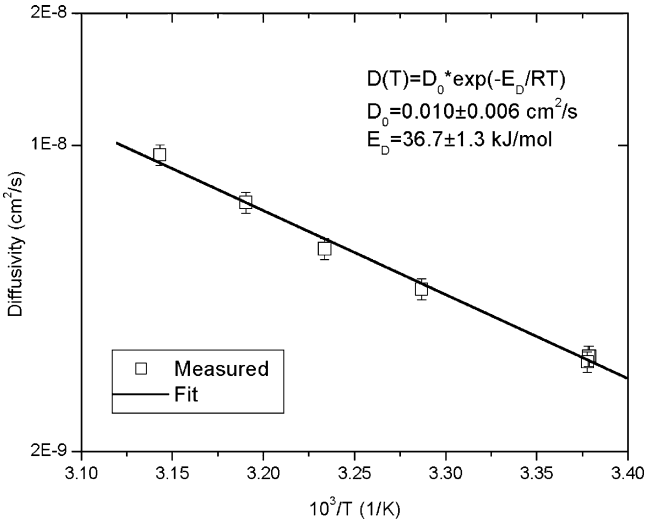

Fig. 6. Temperature dependence of CO_2 diffusivity in PLA (*L*:*D* = 98.7:1.3).

30 °C, CO_2 solubility is 0.025 cm^3 (STP)/cm^3 (polymer) cmHg. The activation energy is negative, and the value is −18.2 kJ/mol. The independent CO_2 diffusivity and solubility in PLA have never been reported before, so a direct comparison with literature values is not possible. For PLA with different *L*/*D* ratios, CO_2 permeation behaves almost the same way as PLA with *L*:*D* = 98.7:1.3.

3.5. O_2 permeation

Fig. 8 shows time-lag plot for O_2 permeation in PLA (*L*:*D* = 80:20) at 22.8 °C. The membrane thickness is 50.0 μm. The time lag is about 150 s, an order of magnitude lower compared to that of CO_2. The measured permeability is 0.14 Barrer, diffusivity is 3.6×10^{-8} cm^2/s, and solubility is 3.8×10^{-4} cm^3 (STP)/cm^3 (polymer) cmHg. Again, the permeability is close to values from other sources. The permeation activation energy is 24.9 kJ/mol.

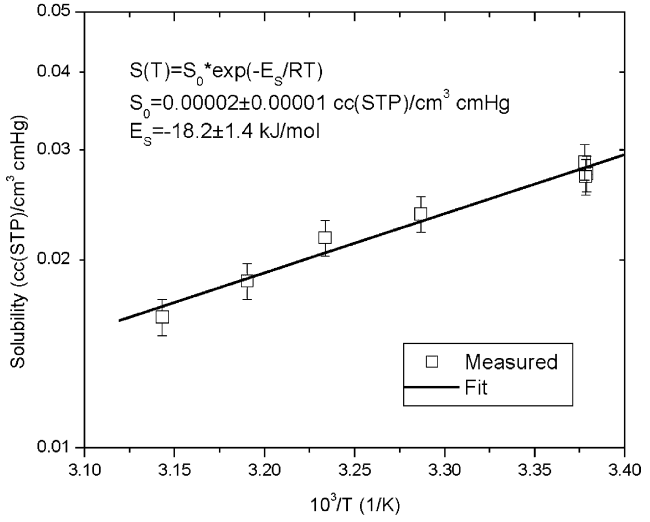

Fig. 7. Temperature dependence of CO_2 solubility in PLA (*L*:*D* = 98.7:1.3).

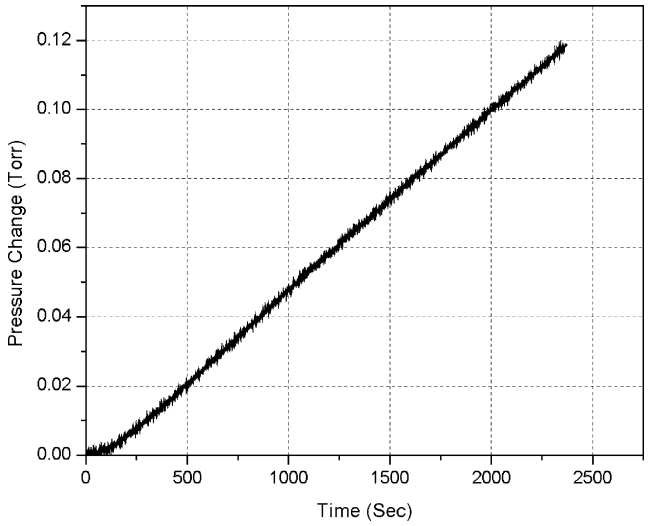

Fig. 8. Time-lag plot for O_2 permeation in PLA (*L*:*D* = 80:20). Temperature is 22.8 °C.

3.6. N_2 permeation

It is well known that N_2 has lower diffusivity and permeability compared to O_2 in most polymer films, which serves as the basis of air separation. PLA behaves as expected; the measured N_2 permeability in PLA (*L*:*D* = 98.7:1.3) is about 0.05 Barrer, 5 times smaller than O_2. This small permeation is difficult to measure accurately. The time lags are only a few seconds for all the films of thickness around 50 μm, so accurate measurement of diffusivity is very difficult. One way to solve this problem is to increase the film thickness. Measurements were done using PLA (*L*:*D* = 80:20) film with thickness of 154.0 μm. It was found that even with increased film thickness, the time lag is still very short and hard to get meaningful diffusivity data. The problem associated with increased film thickness is that the permeation becomes so low that permeability becomes hard to measure. Thus, for N_2, it was not possible to measure separate diffusivity and solubility contributions to the permeability with time-lag method.

3.7. Discussion

Table 2 summarizes the results for N_2, O_2 and CO_2 permeation properties (permeability, diffusivity and solubility) in PLAs with three different *L*/*D* ratios. The activation energies are listed in Table 3. The values reported in Table 2 deserve further comment.

Error analysis of the time-lag apparatus reveals that for CO_2 permeation, the maximum uncertainties of the given results for permeability, diffusivity and solubility are about 4%, 6% and 7%, respectively. For O_2 permeation, the values increase to 7%, 12% and 14%. For N_2 permeation, the values are 7%, 16% and 18%. The major source of uncertainty is from the nonuniformity of the membrane thickness. Another measurement issue is the inherent system leaks. For CO_2 permeation, the system leak rate (around 10^{-8} cm^3/s) is much smaller than the permeation, and with the long time lag, both permeability and diffusivity can be measured accurately. However, for N_2, the permeation rate is

Table 2
Summary of PLA permeation properties

Gas	*L*:*D* ratio	P_θ (30°C) (Barrer)	D_θ (30°C) (cm^2/s)	S_θ (30°C) (cm^3 (STP)/cm^3 (polymer) cmHg)
CO_2	98.7:1.3	1.10	4.4E−9	0.025
	80:20	0.51	3.8E−9	0.013
	50:50	0.71	4.5E−9	0.016
O_2	98.7:1.3	0.26	5.7E−8	4.9E−4
	80:20	0.18	5.6E−8	3.2E−4
	50:50	0.17	7.6E−8	2.2E−4
N_2	98.7:1.3	0.05	2.4E−8	2.2E−4
	80:20	0.02	[a]	[a]
	50:50	0.03	[a]	[a]

[a] Not available.

very small, so the leaking becomes significant and results in less accurate permeability measurements. Also the very short time lag makes it harder to get accurate measurements of diffusivity. That is the reason why some diffusivity data are not reported in Table 2.

The new permeability data are about one order of magnitude lower than the previously reported results [8], but much closer to the reported permeability of biaxially oriented films [6,7]. Even the present pre-annealed films show much lower permeation than previously reported. One possible explanation is that previous results were obtained using a flow through system with gas chromatography detection necessitating the use of very thin PLA films-only about 5 μm in thickness. Such a thin film is very hard to handle, some structural defects such as pinholes could be formed in the film. These thin films were not annealed. Also, the presence of the helium carrier gas may have affected the permeation. Finally, the small permeation rates may have caused problems in the legitimacy of the GC calibration curves.

Since no diffusivity and solubility data for PLA have ever been reported, the results reported here represent new findings. The additional solubility measurements made by quartz crystal microbalance (QCM) can be used for comparison [12]. Larger discrepancies exist between them and solubility values determined by time-lag methods. For CO_2, the difference is small, the QCM gives solubility about two to three times higher than the time-lag results. But for N_2 and O_2, the time-lag method gives solubility value about 25–40 times lower than QCM, which requires additional comment. The exact reason for the discrepancy is not clear. The results of QCM were obtained using a much thinner film coating (2.6 μm). However, at this thickness, the deviation of the Sauerbrey equation will occur [13]. Also the significance of the viscoelastic effects on frequency shifts in the quartz crystal should be considered [14].

Table 3
Activation energy for permeation

Gas	*L*/*D* ratio	E_P (kJ/mol)	E_D (kJ/mol)	E_S (kJ/mol)
CO_2	98.7:1.3	18.1	36.3	−18.4
	80:20	17.8	32.2	−13.9
	50:50	14.3	34.8	−25.4
O_2	98.7:1.3	24.0	42.7	−19.2
	80:20	24.9	40.8	−15.9
	50:50	26.6	68.8	−42.0
N_2	98.7:1.3	34.6	59.3	−25.0
	80:20	40.9	[a]	[a]
	50:50	35.0	[a]	[a]

[a] Not available.

Finally, as all of the samples were solution cast and are amorphous, the effect of optical composition on amorphous phase permeability is small and effectively negligible. It should be remembered though that optical composition does strongly affect achievable crystallinity in melt processing operations. Under such conditions, permeability should be dominated by the level of crystallinity in the samples although the density of amorphous and crystalline PLA is not very different.

4. Conclusions

Due to the discrepancy of previous permeability results and newer literature values, gas permeation properties of PLA were revisited using the time-lag method. It was found that annealing the PLA film is necessary for path independent and reproducible results. New permeability values are lower than previous reported. Separate contributions of the pure gas diffusivities and solubilities in PLA are reported for the first time. The PLA optical composition has a very small effect on permeation properties confirming previous results.

Acknowledgements

Funding was provided by the EPA/NSF Technology for a Sustainable Environment Program (no. R 826733-01-0) and by the Agriculture Industries of the Future Program of the Office of Industrial Technologies, U.S. Department of Energy.

References

[1] M.H. Hartman, High molecular weight polylactic acid polymers, in: D.H. Kaplan (Ed.), Biopolymers from Renewable Resources, Springer-Verlag, Berlin, 1998, pp. 367–411.
[2] J.R. Dorgan, Polylactides: properties and prospects of an environmentally benign plastic from renewable resources, Macromol. Symp. 175 (2001) 55–66.
[3] J. Lunt, Poly(lactic acid) polymers for fibers and nonwovens, Int. Fiber J. (2000) 48–52.

[4] R. Auras, B. Harte, S. Selke, An overview of polylactides as packing materials, Macromol. Biosci. 4 (2004) 835–864.
[5] G.L. Siparsky, K.J. Voorhees, J.R. Dorgan, K. Schilling, Water transport in poly(lactic acid), poly(lactic acid-*co*-caprolactone) copolymers, and poly(lactic acid)/polyethylene glycol blends, J. Environ. Polym. Degrad. 5 (1997) 125–136.
[6] R.A. Auras, B. Harte, S. Selke, R.J. Hernandez, Mechanical, physical, and barrier properties of poly(lactide) films, J. Plast. Film Sheet. 19 (2003) 123–135.
[7] NaturalWorks PLA Polymer 4042D Biaxially oriented films—general purpose. Technical data sheet, Naturalworks, LLC, Minneapolis, MN, USA, 2006.
[8] H.J. Lehermeier, J.R. Dorgan, J.D. Way, Gas permeation properties of poly(lactic acid), J. Membr. Sci. 190 (2001) 243–251.
[9] D. Hands, Permeability, in: R. Brown (Ed.), Handbook of Polymer Testing, Physical methods, New York, 1999, pp. 747–760 (Chapter 30).
[10] J. Brandrup, E.H. Immergut, E.A. Grullce, Polymer Handbook, John Wiley & Sons, New York, 1999.
[11] K. Nagai, L.G. Toy, B.D. Freeman, et al., Gas permeability and hydrocarbon solubility of poly[1-phenyl-2-[*p*[-triisopropylsilyl)phenyl]acetylene], J. Polym. Sci. B: Polym. Phys. 38 (2000) 1474–1484.
[12] N.S. Oliveira, J. Oliveira, T. Gomes, A. Ferreira, J. Dorgan, I.M. Marrucho, Gas sorption in poly(lactic acid) and packing materials, Fluid Phase Equilibr. 222/223 (2004) 317–324.
[13] B.D. Vogt, E.K. Lin, W-L. Wu, C.C. White, Effect of film thickness on the validity of the Sauerbrey equation for hydrated polyelectrolyte films, J. Phys. Chem. B 108 (2004) 12685–12690.
[14] L. Banda, M. Alcoutlabi, G.B. McKenna, Errors induced in quartz crystal mass uptake measurement by nongravimetric effects: considerations beyond the EerNisse caution, J. Polym. Sci. B: Polym. Phys. 44 (2006) 801–814.